Chemical Reactivity of Oxo- and Aza-γ-lactam Rings

by **Gabriela L. Borosky**[a]) and **Francisco Muñoz***[b])

[a]) Unidad de Matemática y Física, Facultad de Ciencias Químicas, Universidad Nacional de Córdoba, Ciudad Universitaria, 5000 Córdoba, Argentina

[b]) Departament de Química, Universitat de les Illes Balears, Ctra. Valldemosa km 7.5, E-07071 Palma de Mallorca

Different mechanisms for the alkaline hydrolysis of oxo and aza-γ-lactam rings have been studied by *ab initio* calculations at the MP2/6-31 + G*//MP2/6-31 + G* and B3LYP/6-31 + G*//B3LYP/6-31 + G* levels. The tetrahedral intermediate can undergo two different reactions, the cleavage of the C_2-N_2 bond (the classical mechanism) and the cleavage of the C_2-X_6 bond (X=O, N). Both compounds present similar energy barriers for the classical fragmentation, and show considerably lower barriers for the alternative mechanism. Because of this reactivity, the compounds studied are expected to be β-lactamase inhibitors.

Introduction. – β-Lactam antibiotics constitute one crucial landmark in the history of medicine. Since the discovery of penicillin at the end of the 1920s, β-lactam antibiotics have been widely used in the treatment of bacterial diseases [1].

One of the major constraints to the biological action of β-lactam antibiotics lies in the occurrence of β-lactamases that inactivate them by hydrolyzing the lactam ring before they can reach carboxypeptidases and transpeptidases, enzymes involved in the synthesis of the bacterial cell walls [2].

The increase of the bacterial resistance against β-lactam action has promoted renewed efforts to find new molecules with antibacterial activity. Thus, carbapenens, cephamycins, oxacephamycins, and γ-lactam antibiotics have been proposed as effective compounds against bacteria and stable to the action of the β-lactamases. In the γ-lactam antibiotics, the β-lactam ring has been replaced by a pyrazolidinone ring [3–6].

Nangia and co-workers [7–9] proposed that aza-β-lactam compounds must possess antibacterial activity. Theoretical calculations of oxo- and aza-β-lactam structures led to the conclusion that such structures can also possess inhibitory activity against β-lactamases [10][11].

In this work, we report various potential mechanisms for the alkaline hydrolysis of oxo- and aza-γ-lactam structures (*Scheme*) where the CHR group at position 6 (next to the C=O group) was replaced with an O-atom or a N–NH–CHO group. Two different mechanisms have been considered: *a*) The classical mechanism, which involves the formation of the tetrahedral intermediate and subsequent cleavage of the C_2-N_3 bond [12–15]. *b*) An alternative mechanism involving cleavage of the C_2-X_6 bond in the tetrahedral intermediate.

Methodology. – The *ab initio* calculations were carried out at the MP2/6-31 + G*// MP2/6-31 + G* [16][17] and B3LYP/6-31 + G*//B3LYP/6-31 + G* [18–20] levels.

Scheme

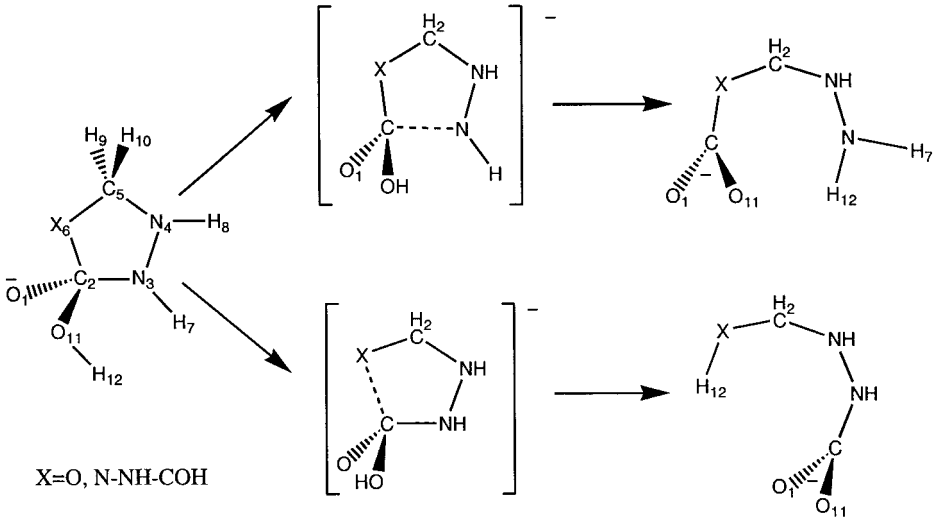

Henceforward, MP2 and B3LYP stand for MP2/6-31 + G*//MP2/6-31 + G* and B3LYP/6-31 + G*//B3LYP/6-31-G*, respectively.

All the transition states were characterized by B3LYP calculations by exhibiting just one imaginary frequency, greater than 100i cm^{-1} in all cases. To confirm the transition states proposed in this work, we performed IRC calculations of those structures. All the energetic minima showed no imaginary frequencies.

The calculations were performed on a *SGI Origin 200* computer running the *Gaussian 94* [21] and *98* [22] programs.

Results and Discussion. – The alkaline hydrolysis of compounds derived from the pyrazolidinone ring through a B_{AC2} mechanism has been studied. This process involves a nucleophilic attack of a OH^- anion on the γ-lactam C=O group, further formation of a tetrahedral intermediate, cleavage of the C_2-N_3 bond, and subsequent H transfer to N_3. Alternatively, the fragmentation of the bond between C_2 and the atom at the 6-position of the ring has been calculated for the tetrahedral intermediate. As formation of this intermediate takes place without activation energy in the gas phase, reactions were considered starting from this structure [15][23]. The derivatives studied were those having at the 6-position an O-atom or a N-atom substituted by a NH−COH group. The mechanism and the numbering of the system are depicted in the *Scheme*.

Transition states for the ring-opening pathways presented just one imaginary frequency at which the atoms of the bond being cleaved were involved, and these structures were further confirmed by IRC calculations. B3LYP Activation barriers were lower than the MP2 ones, as is usually observed. Reaction energies are presented in *Tables 1* and *2*.

Oxo Compound. For the compound with the O-atom at the 6-position, transfer of the proton of the OH group occurred in a concerted manner for both fragmentation

Table 1. *Total Energies* [hartree] *for the Species Involved in the Ring-Opening Reactions of the Tetrahedral Intermediate of the Pyrazolidinone Derivatives*

X		**a** or **a′**	**b** or **b′**	**d** or **d′**	**c** or **c′**	**e** or **e′**	**g′**
O	B3LYP	– 414.40255	– 414.37698	– 414.39955	– 414.46027	– 414.46955	–
	MP2	– 413.25370	– 413.21956	– 413.24625	– 413.30477	– 413.31467	–
	Imag. freq. [cm^{-1}]	0	1 (288.91*i*)	1 (151.55*i*)	0	0	–
	ZPE[a])	0.08868	0.08630	0.08746	0.08963	0.08774	–
N–NH–COH	B3LYP	– 563.20716	– 563.18259	– 563.19409	– 563.26502	– 563.22722	– 563.25111
	MP2	– 561.62786	– 561.59750	– 561.60387	– 561.68064	– 561.63488	– 561.63488
	Imag. freq. [cm^{-1}]	0	1 (200.90*i*)	1 (85.73*i*)	0	0	0
	ZPE[a])	0.12719	0.12447	0.12508	0.12819	0.12612	0.12830

[a]) At the B3LYP level.

pathways of the tetrahedral intermediate, yielding a carboxylate anion. An intramolecular H-bond between the transferred H-atom and the closest of the O-atoms of the carboxylate were observed in both cleavage products. The calculated structures are shown in *Fig. 1* and geometrical parameters are given in *Table 3*. In general, the MP2 calculations lengthened the bond distances by up to *ca*. 0.01 Å, but the most important modification was the decrease of the C_2-O_6 bond by 0.027 Å in the tetrahedral intermediate. H-Bond distances varied also by more than 0.01 Å. The reaction profiles are displayed in *Figs. 2* and *3*. The MP2 calculations raised the barriers and slightly diminished the exothermicity of the fragmentation pathways. The tetrahedral intermediate conformation (**a** in *Fig. 1*) that evolves through the transition states for both fragmentation pathways is the one generated by attack of the OH^- ion on the upper face of the ring that has H_7- and H_8-atoms at the equatorial (down)-axial (down) position. The transition state for the C_2-N_3 fragmentation, **b**), was characterized by a distance of 2.269 Å at the B3LYP level and of 2.265 Å by the MP2 calculations. The proton involved was located by 1.797 Å and 1.749 Å from N_3, respectively, this short

Table 2. *Energies* [kcal/mol] *for the Ring Opening of the Tetrahedral Intermediate of the Pyrazolidinone Derivatives*

X		C_2-N_3 cleavage		C_2-X_6 cleavage	
		$\Delta H^{\neq}$	ΔH_r	$\Delta H^{\neq}$	ΔH_r
O	B3LYP	16.04	– 36.22	1.88	– 42.04
	B3LYP[a])	14.55	– 35.62	1.11	– 42.63
	MP2	21.42	– 32.04	4.67	– 38.26
N–NH–COH	B3LYP	15.42	– 36.30	8.20	– 12.59 – 27.58[b])
	B3LYP[a])	13.71	– 35.67	6.88	– 13.26 – 26.88[b])
	MP2	19.03	– 33.12	15.05	– 4.40 – 22.68[b])

[a]) Including zero-point vibrational contribution. [b]) Product with H transferred (**g′** in *Fig. 4*).

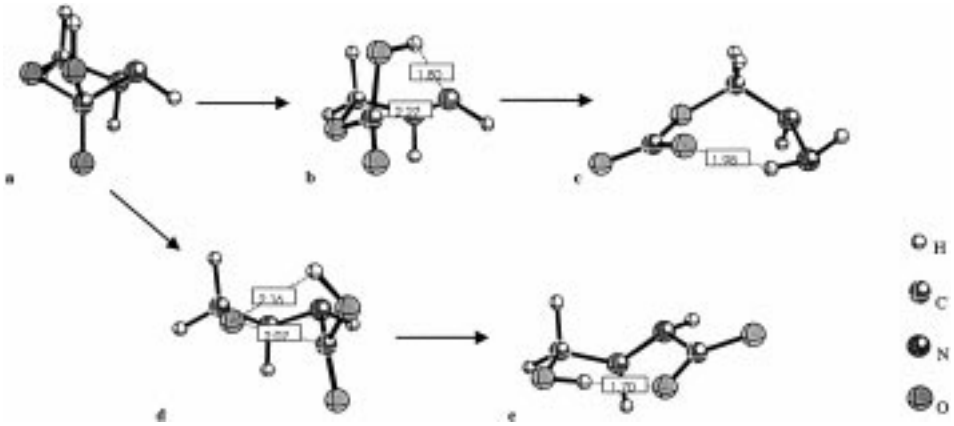

Fig. 1. *Structures corresponding to the oxo compound*. **a**: Tetrahedral intermediate; **b**: transition state for the C_2-N_3 cleavage; **c**: product for the C_2-N_3 cleavage; **d**: transition state for the C_2-O_6 cleavage; **e**: product for the C_2-O_6 cleavage.

Table 3. *Main Geometric Parameters for the Oxo-Compound Structures in* Fig. 1[a])

	Structure **a**		Structure **b**		Structure **c**		Structure **d**		Structure **e**	
	B3LYP	MP2	B3LYP	MP2	B3LYP	MP2	B3LYP	MP2	B3LYP	MP2
O_1C_2	1.2593	1.2690	1.2243	1.2278	1.2359	1.2425	1.2273	1.2304	1.2504	1.2569
C_2N_3	1.5298	1.5254	2.2688	2.2652	3.4014	3.3678	1.4821	1.4758	1.4542	1.4570
N_3N_4	1.4542	1.4571	1.4603	1.4619	1.4478	1.4499	1.4496	1.4522	1.4238	1.4275
N_4C_5	1.4702	1.4656	1.4402	1.4375	1.4584	1.4552	1.4942	1.4904	1.4540	1.4502
C_5O_6	1.4018	1.4158	1.4398	1.4437	1.4189	1.4236	1.3599	1.3673	1.4168	1.4243
C_2O_6	1.5952	1.5680	1.3967	1.3988	1.4614	1.4690	2.0677	2.1418	3.3253	3.3252
C_2O_{11}	1.4274	1.4306	1.3889	1.3879	1.2563	1.2625	1.3793	1.3750	1.2690	1.2745
$O_{11}H_{12}$	0.9715	0.9764	0.9978	1.0090	1.9768	2.0135	0.9760	0.9878	1.7041	1.7331
O_6H_{12}	2.3852	2.3527	2.6144	2.6008	2.7598	2.6833	2.1568	1.9866	1.0036	1.0021
N_3H_{12}	2.4079	2.4052	1.7971	1.7488	1.0284	1.0281	2.4438	2.4428	2.6504	2.6253
N_4H_{12}	3.5210	3.5322	2.7753	2.7337	2.0191	2.0186	3.3936	3.3258	2.4068	2.3946

[a]) Bond lengths in Å.

distance implying the existence of an intramolecular H-bond. For the C_2-O_6 fragmentation, the distance between these atoms in the transition state **d** was 2.068 Å according to the B3LYP calculations and 2.142 Å according to MP2. The intramolecular H-bond involved had a distance of 2.157 Å and 1.987 Å to O_6, respectively.

Activation energies showed that the C_2-O_6 cleavage is the most likely process, as the energy differences in the barriers were very notorious, 14.16 kcal/mol at the B3LYP/6-31 + G* level and 16.75 kcal/mol at the MP2/6-31 + G* level (*Figs. 2* and *3*). This observation could be rationalized by the negative charge density that develops in the transition state at the atom whose bond with C_2 is cleaved being better borne by the more electronegative O-atom than by the N-atom. Furthermore, the greater basicity of O-atom should facilitate the H transfer, which reflects in the greater exothermicity of the C_2-O_6 cleavage. The very low barrier afforded for the C_2-O_6

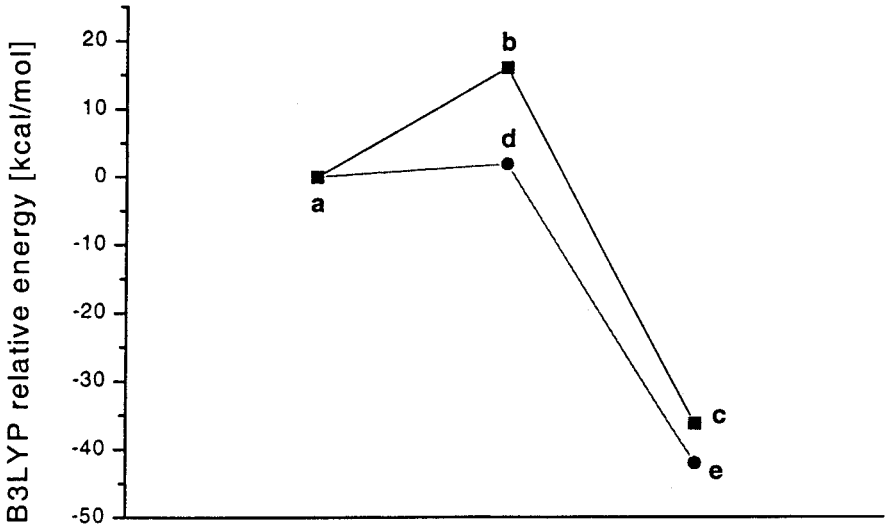

Fig. 2. *B3LYP Reaction profile for the fragmentation pathways for alkaline hydrolysis of the oxo compound*

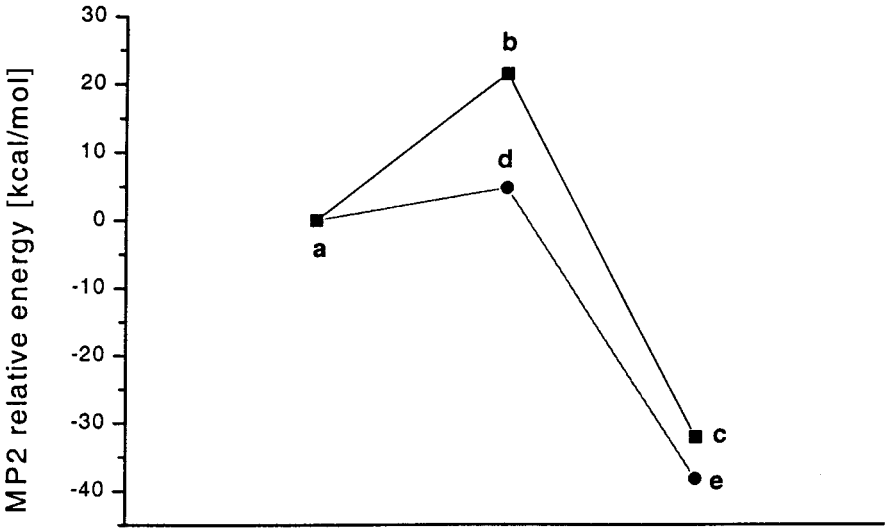

Fig. 3. *MP2 Reaction profile for the fragmentation pathways for alkaline hydrolysis of the oxo compound*

cleavage indicates that this process would take place at room temperature at a high rate.

Aza Compound. With the N-atom at the 6-position, the tetrahedral intermediate conformation that is connected to the transition states for both fragmentation pathways is the one generated by attack of the OH^- ion on the upper face of the ring that has the H_7- and H_8-atoms at the equatorial (down)-axial (down) position. The calculated

structures are shown in *Fig. 4*, and geometrical parameters are given in *Table 4*. Variations in bond distances between B3LYP and MP2 calculations were more notorious in H-bonds, although the decrease by 0.027 Å in the C_2-N_6 bond in the tetrahedral intermediate should be noted. It is noteworthy that, in the tetrahedral intermediate, C_2-N_6 distance is slightly longer than the C_2-N_3 distance, suggesting an easy C_2-N_6 bond fission.

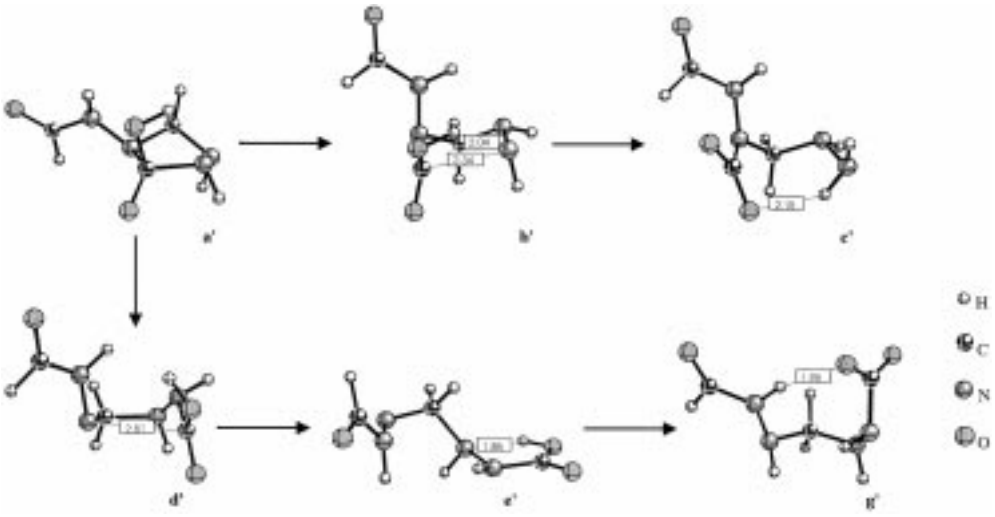

Fig. 4. *Structures corresponding to the aza compound*. **a′**: Tetrahedral intermediate; **b′**: transition state for the C_2-N_3 cleavage; **c′**: product for the C_2-N_3 cleavage; **d′**: transition state for the C_2-N_6 cleavage; **e′**: product for the C_2-N_6 cleavage; **g′**: product with the H-atom transferred.

Table 4. *Main Geometric Parameters for the Aza-Compound Structures in* Fig. 4[a])

	Structure **a′**		Structure **b′**		Structure **c′**		Structure **d′**		Structure **e′**		Structure **g′**	
	B3LYP	MP2	B3LYP	MP2	B3LYP	MP2	B3LYP	MP2	B3LYP	MP2	B3LYP	MP2
O_1C_2	1.2606	1.2694	1.2222	1.2270	1.2429	1.2517	1.2141	1.2177	1.2208	1.2265	1.2396	1.2472
C_2N_3	1.5431	1.5365	2.3438	2.3751	3.2262	3.0854	1.4249	1.4107	1.3843	1.3904	1.4834	1.4778
N_3N_4	1.4603	1.4656	1.4448	1.4466	1.4496	1.4496	1.4292	1.4271	1.4231	1.4280	1.4217	1.4252
N_4C_5	1.4582	1.4586	1.4721	1.4724	1.4772	1.4729	1.5507	1.5508	1.5567	1.5347	1.4561	1.4544
C_5N_6	1.4634	1.4614	1.4701	1.4679	1.4443	1.4450	1.4147	1.4136	1.4046	1.4111	1.4829	1.4792
C_2N_6	1.5756	1.5490	1.4683	1.4584	1.4983	1.4998	2.8086	2.8769	4.5406	4.4366	3.4876	3.4358
C_2O_{11}	1.5026	1.5116	1.3744	1.3715	1.2573	1.2634	1.3634	1.3721	1.3508	1.3539	1.2704	1.2777
$O_{11}H_{12}$	0.9709	0.9760	0.9880	0.9990	2.1529	2.1921	0.9749	0.9788	0.9983	1.0036	3.8532	3.8580
N_6H_{12}	2.8764	2.8977	2.6141	2.5503	2.8679	2.8748	3.1081	3.2940	4.8476	4.2467	1.0199	1.0217
N_3H_{12}	2.1375	2.1216	2.0388	1.9842	1.0270	1.0270	2.2905	2.2749	2.1420	2.1386	2.8751	2.8526
N_4H_{12}	3.2309	3.2044	2.9931	2.9660	2.0238	2.0262	3.5728	3.6067	1.8654	1.8373	2.6225	2.6076

[a]) Bond lengths in Å.

Reaction profiles are shown in *Figs. 5* and *6*. Activation energies were higher, and exothermicities were lower by the MP2 calculations, especially for the C_2-N_6 cleavage, as it will be remarked below. The C_2-N_3 cleavage occurred with transfer of the acidic proton to yield the carboxylate anion, and a H-bond interaction was observed in the

product between the transferred H-atom and the carboxylate group. The C_2-N_3 bond length in the transition state (**b′** in *Fig. 4*) was 2.344 Å by B3LYP and 2.375 Å according to MP2, the H-bond distance being 2.039 Å and 1.984 Å, respectively. The activation energies and heats of reaction calculated with both methods were similar to those of the oxo compound.

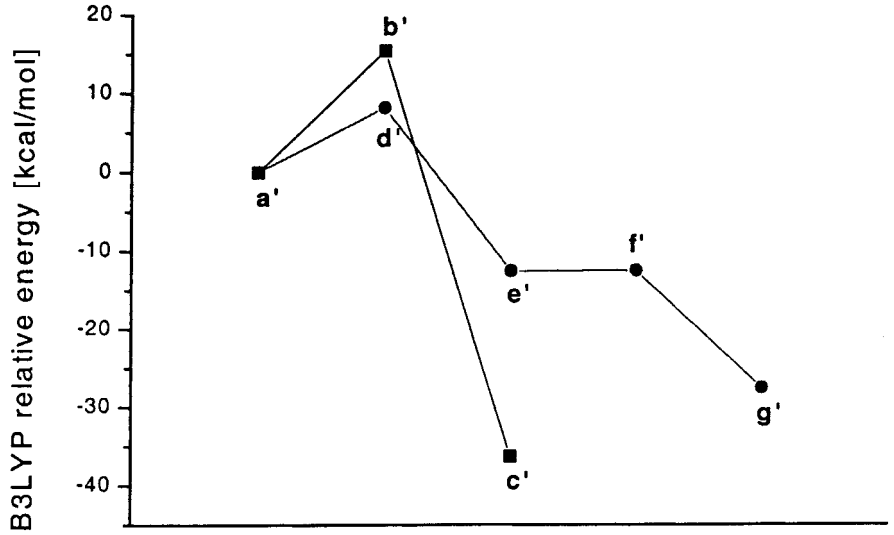

Fig. 5. *B3LYP Reaction profile for the fragmentation pathways for alkaline hydrolysis of the aza compound*

However, for the C_2-N_6 cleavage, the transition state (**d′**) was located at a distance of 2.809 Å according to B3LYP and 2.877 Å by MP2, *i.e.*, at a longer distance than for the C_2-O_6 analog. The process took place without transfer of the proton, *i.e.*, the transition structure was not H-bond-stabilized, generating a higher barrier and a lesser exothermicity than with oxygen. Nevertheless, this would be the kinetically preferred path for the nitrogen compound, even when it is the thermodynamically less favored. Conjugation within the $N_6-C_5-N_4$ system can be inferred according to the bond lengths, which go from 1.463 Å and 1.458 Å for the N_6-C_5 and C_5-N_4 distances in the tetrahedral intermediate to 1.405 Å and 1.557 Å, respectively, in the open product (B3LYP results, structure **e′**, *Fig. 4*), as well as for the development of negative charge at the N_4-atom upon fragmentation. At the MP2 level, these distances went from 1.461 Å and 1.459 Å to 1.411 Å and 1.535 Å, respectively. The stability brought about by resonance of the resulting anion could be responsible for the absence of a concerted proton transfer in this fragmentation path. A H-bond interaction was observed between the proton of the OH group and the N_4-atom.

The product for the C_2-N_6 fragmentation with the H-atom transferred to the N_6-atom was also calculated (**g′**). This structure presents a H-bond between the closest O-atom of the carboxylate group and one H-atom of the rest attached to the N_6-atom. As this product has a lower energy than that described above, the intermediate **e′** would yield **g′** through an intramolecular proton-transfer step. Although the transition state for this process was not calculated (**f′**, *Figs. 5* and *6*), the activation barrier is expected

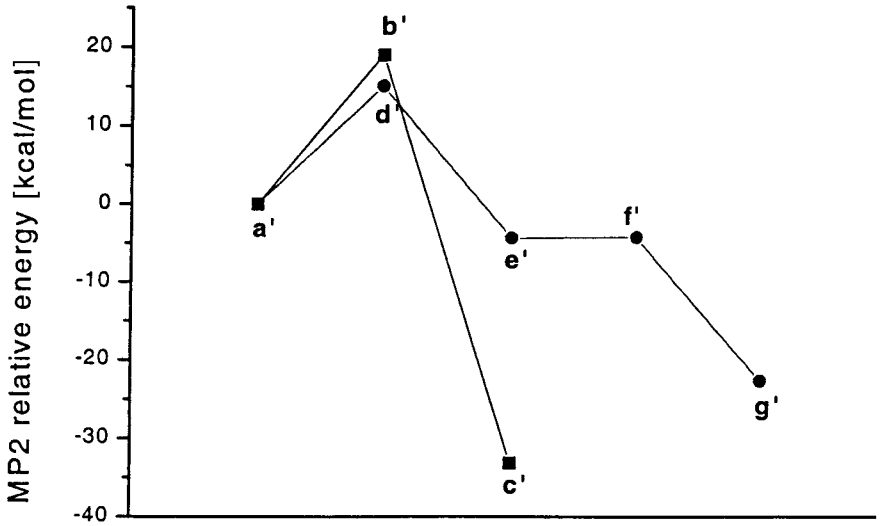

Fig. 6. *MP2 Reaction profile for the fragmentation pathways for alkaline hydrolysis of the aza compound*

to be very low [10][11]. In this way, formation of **g′** would increase the exothermicity of the whole C_2-N_6 fragmentation pathway.

On the basis of the results presented, the alkaline hydrolysis of both the oxo and the aza compounds will yield preferentially the products arising from the nonclassical cleavage of the C_2-X_6 bond. Accordingly, these structures could act as inhibitors of β-lactamases. β-Lactamases degrade β-lactam antibiotics by catalyzing the hydrolysis of the ring, forming an acyl-enzyme complex (in some way, similar to the structures **a** and **a′** [12]) that releases inert β-amino acids upon H_2O attack. Because of their reactivity, the compounds under study would be expected to form first an acyl-enzyme complex that evolves through C_2-X_6 bond fragmentation to a new especially stable acyl-enzyme complex that would not hydrolyze. This observation would provoke the blockage of the enzyme, as it is the case for clavulanic acid, a known inhibitor of β-lactamases.

This work is a part of a research project supported by *Spanish DGICYT* (project PB96-0596-C02). *G. L. B.* is grateful to the *Programa de Cooperación Interuniversitaria* which allowed her to realize this work.

REFERENCES

[1] R. B. Chamber,'Chemistry and Biology of β-Lactam Antibiotics', Academic Press, New York, 1982, Vol. 3, pp. 287–300.
[2] J. R. Knowles, *Acc. Chem. Res.* **1985**, *18*, 97.
[3] D. B. Boyd, *J. Med. Chem.* **1993**, *36*, 1443.
[4] L. D. Jungheim, S. K. Sigmund, J. W. Fisher, *Tetrahedron Lett.* **1987**, *28*, 285.
[5] R. J. Ternansky, S. E. Draheim, *J. Med. Chem.* **1993**, *36*, 3219.
[6] R. J. Ternansky, S. E. Draheim, A. J. Pike, F. T. Counter, J. A. Eudaly, J. S. Kasher, *J. Med. Chem.* **1993**, *36*, 3224.
[7] A. J. Nangia, *J. Mol. Struct. (THEOCHEM)* **1991**, *251*, 237.
[8] A. J. Nangia, P. S. Chandrakala, P. V. Balaramakrishma, T. V. Latta, *J. Mol. Struct. (THEOCHEM)* **1995**, *343*, 157.

[9] P. S. Chandrakala, A. K. Katz, H. L. Carrell, P. R. Sailaja, A. R. Podile, A. J. Nangia, G. R. Desinaju; *J. Chem. Soc., Perkin Trans 1* **1998**, 2597.
[10] M. Coll, J. Frau, F. Muñoz, J. Donoso, *J. Phys. Chem A* **1998**, *102*, 5915.
[11] M. Coll, J. Frau, B. Vilanova, J. Donoso, F. Muñoz, F. García Blanco, *J. Phys. Chem. A* **1999**, *103*, 8879.
[12] J. Frau, J. Donoso, F. Muñoz, F. García Blanco, *J. Comput. Chem*. **1992**, *13*, 681.
[13] Y. G. Smeyers, A. Hernández-Laguna, R. González-Jonte, *J. Mol. Struct. (THEOCHEM)* **1993**, *287*, 261.
[14] J. J. Pranata, *J. Phys. Chem*. **1994**, *98*, 1180.
[15] J. Frau, J. Donoso, F. Muñoz, F. García Blanco, *Helv. Chim. Acta* **1996**, *79*, 353.
[16] J. A. Pople, J. S. Binkley, R. Seeger, *Int. J. Quantum Chem*. **1977**, *510*, 1.
[17] J. A. Pople, R. Seeger, R. Krishman, *Int. J. Quantum Chem*. **1977**, *511*, 165.
[18] A. D. Becke, *J. Chem. Phys.* **1993**, *98*, 5648.
[19] C. Lee, W. Yang, R. G. Parr, *Phys. Rev. B* **1989**, *37*, 785.
[20] B. Meihlich, A. Savin, H. Stoll, H. Preuss, *Chem. Phys. Lett*. **1989**, *157*, 200.
[21] M. J. Frisch, G. W. Trucks, H. B. Schlegel, P. M. W. Gill, B. G. Johnson, M. A. Robb, J. R. Cheeseman, T. A. Keith, H. B. Petersson, J. A. Montgomery, B. Raghavachari, M. A. Al-Laham, V. G. Zakrzewski, J. V. Otiz, J. B. Foresman, J. Cioslowski, B. B. Stefanov, A. Nanayakkara, M. Challacombe, C. Y. Peng, P. Y. Ayala, W. Chen, M. W. Wong, J. L. Andres, E. S. Replogle, R. Gomperts, R. L. Martin, D. J. Fox, J. S. Binkley, D. J. Defrees, J. Baker, J. P. Stewart, M. Head-Gordon, C. Gonzalez, J. A. Pople, *Gaussian 94, Rev. D.1, Gaussian Inc.*, Pittsburgh, P.A., 1995.
[22] M. J. Frisch, G. W. Trucks, H. B. Schlegel, G. E. Scuseria, M. A. Robb, J. R. Cheeseman, V. G. Zakrzewski, J. A. Montgomery, R. E. Stratmann, J. C. Burant, S. Dapprich, J. M. Millam, A. D. Daniels, K. N. Kudin, M. C. Strain, O. Farkas, J. Tomasi, V. Barone, M. Cossi, R. Cammi, B. Mennucci, C. Pomelli, C. Adamo, S. Clifford, J. Ochterski, G. A. Petersson, P. Y. Ayala, Q. Cui, K. Morokuma, D. K. Malick, A. D. Rabuck, K. Raghavachari, J. B. Foresman, J. Cioslowski, J. V. Ortiz, B. B. Stefanov, G. Liu, A. Liashenko, P. Piskorz, I. Komaromi, R. Gomperts, R. L. Martin, D. J. Fox, T. Keith, M. A. Al-Laham, C. Y. Peng, A. Nanayakkara, C. Gonzalez, M. Challacombe, P. M. W. Gill, B. Johnson, W. Chen, M. W. Wong, J. L. Andres, C. Gonzalez, M. Head-Gordon, E. S. Replogle, J. A. Pople, *Gaussian 98*, *Gaussian, Inc.*, Pittsburgh PA, 1998.
[23] J. Frau, J. Donoso, F. Muñoz, B. Vilanova, F. Garcia Blanco, *Helv. Chim. Acta* **1997**, *80*, 739.

Received October 23, 2000